Interplay of drug-polymer interactions and release performance for HPMCAS-based amorphous solid dispersions

Pradnya Bapat,[1] Shubhajit Paul,[2], Yin-Chao Tseng,[2] Lynne S. Taylor.[1]*

1. Department of Industrial and Physical Pharmacy, College of Pharmacy, Purdue University, West Lafayette, Indiana 47907, United States

2. Material and Analytical Sciences, Research and Development, Boehringer Ingelheim Pharmaceuticals, Inc., Ridgefield, Connecticut 06877, United States

*Correspondence: Lynne S. Taylor

Telephone: +1-765-496-6614; Fax: +1-765-494-6545)

Email address: lstaylor@purdue.edu

Abstract

The interplay between drug and polymer chemistry and its impact on release of the drug from an amorphous solid dispersion (ASD) is a relatively underexplored area. Herein, the release rates of several drugs of diverse chemistry from hydroxypropyl methyl cellulose acetate succinate (HPMCAS)-based ASDs was explored using surface area normalized dissolution. The tendency of the drug to form an insoluble complex with HPMCAS was determined through co-precipitation experiments. The role of pH and the extent of drug ionization was probed to evaluate the role of electrostatic interactions in complex formation. Relationships between the extent of complexation and the drug release rate from an ASD were observed whereby the drugs could be divided into two groups. Drugs with a low extent of insoluble complex formation with HPMCAS tended to be neutral or anionic, and showed reasonable release at pH 6.8 even at higher drug loadings. Cationic drugs formed insoluble complexes with HPMCAS and showed poor release when formulated as an ASD. Thus, and somewhat counterintuitively, a weakly basic drug showed a reduced release rate from an ASD at a bulk solution pH where it was ionized, relative to when unionized. The opposite trend was observed in the absence of polymer for neat amorphous drug. In conclusion, electrostatic interactions between HPMCAS and lipophilic cationic drugs led to insoluble complex formation, which in turn resulted in ASDs with poor release performance.

Keywords: drug-polymer complexation; pH; ionization; solubility

TOC Graphic

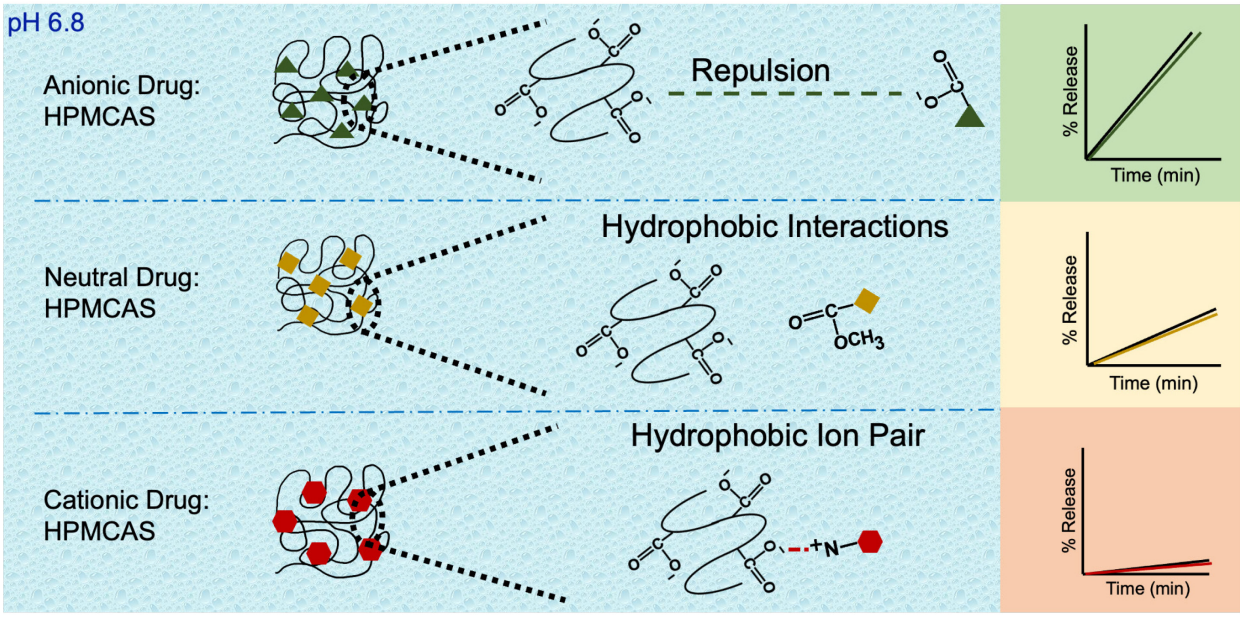
pH 6.8
Anionic Drug:
HPMCAS
Repulsion
% Release
Time (min)
Neutral Drug:
HPMCAS
Hydrophobic Interactions
% Release
Time (min)
Cationic Drug:
HPMCAS
Hydrophobic Ion Pair
% Release
Time (min)

1. Introduction

Amorphous solid dispersion (ASD) formulations are being broadly implemented to address solubility challenges of new chemical entities emerging from pharmaceutical development pipelines.[1–10] An ASD is ideally a molecular mixture of an amorphous drug and a polymer, forming a single phase homogeneous blend. The amorphous form of a drug provides a higher transient solubility compared to equilibrium crystalline solubility, whereby the presence of a polymer of appropriate properties aids crystallization inhibition.[11–14] Polymers also improve the release rate of the drug from the ASD relative to the release rate of neat amorphous drug, specifically for release regimens where both drug and polymer release congruently. This regimen is observed if the release of each component is controlled by the polymer, whereby polymers typically used in ASDs have higher dissolution rates than poorly soluble drugs. Consequently, recent attention has focused on polymer release mechanisms since these, in turn, control drug release. For copovidone-based ASDs, a typical "falling-off-a-cliff" release pattern has been observed for many systems whereby at lower drug loadings, congruent and rapid release of drug and polymer occurs, whereas at higher drug loadings (above the limit of congruency) a drastic drop in drug release rate has been noted, and drug and polymer no longer release together.[15–20] Specific drug-polymer interactions such as hydrogen bonding have been implicated in reduced release rates at relatively low drug loadings.[17,18,21–27] For hydroxypropyl methyl cellulose acetate succinate (HPMCAS)-based ASDs, fewer studies addressing release mechanisms are available. However, it has been noted for some systems that instead of such a drastic drop, there is a more gradual decrease in release rate as a function of drug loading.[14,19,28,29]

Enteric polymers such as HPMCAS have been widely studied in the context of coating rupture mechanisms,[30–37] however, the impact of a molecularly dispersed drug, as in an ASD

formulation, on HPMCAS dissolution has received much less scrutiny. Given that HPMCAS is often the preferred polymer for spray dried ASD formulations,[38–41] this knowledge gap should be addressed in order to optimize ASD formulations, taking into account the increasing molecular diversity of emerging drug candidates. In particular, the role of drug-polymer interactions that persist in the presence of aqueous media should be considered in terms of their impact on release performance. Notably, HPMCAS has the potential to form not only hydrogen bonds,[42] but also ionic interactions with drugs.[43] In a previous study from our group,[14] it was suggested that the poor performance of lumefantrine ASDs with enteric polymers resulted from the formation of drug-polymer ionic interactions which in turn led to reduced polymer hydration and dissolution.

Herein, we explore the hypothesis that lipophilic drug cations lead to reduced HPMCAS solubility via formation of an ionic complex, which in turn leads to poor ASD release performance at even low drug loadings. In contrast, we hypothesize that anionic or neutral drugs have less impact on polymer solubility at comparable drug loadings, and hence can be loaded to higher amounts while still achieving release. Consequently, the objective of this study was to demonstrate that the ionization state and charge of the drug play a critical role in release performance as a function of drug loading for HPMCAS-based ASDs. We selected a variety of model weakly acidic, basic and neutral drugs. HPMCAS-MF grade, an enteric polymer which starts to show increased solubility above pH 5 and dissolution above pH 6 following ionization of carboxylic acid functionalities, was used as the model polymer. Importantly, enteric polymers such as HPMCAS have been shown to have a decreased pH near the polymer-water interface (unstirred water layer) compared to the bulk solution pH as a result of protons liberated during ionization of carboxylic-acid groups.[34–37,44,45] Therefore, the impact of microenvironmental pH on drug-polymer interactions/release also needs to be considered. The extent of insoluble

complex formation for different drug-HPMCAS combinations was determined at a pH corresponding to that estimated at the polymer-solvent interface for the corresponding buffer system. Release studies were performed at a bulk pH of 6.8 analyzing both drug and polymer release rate. For select systems, release studies were carried out at other (pH 7.5, 9.0) pH values.

2. Materials

Indomethacin (IND) and ritonavir (RTV) were purchased from ChemShuttle (Jiangsu, China). Indomethacin methyl ester (INDester) was synthesized as described previously.[46] Cilnidipine (CIL) was supplied by Euroasia Chemicals Pvt. Ltd. (Mumbai, India). Loratadine (LOR) was purchased from Attix Pharmaceuticals (Toronto, ON, Canada). Phenolphthalein (PHPH) and clotrimazole (CLO) were supplied by Sigma-Aldrich (St. Louis, MO, USA). Cinnarizine (CNZ) was purchased from Alfa Aesar (Ward Hill, MA, USA). Hydroxypropyl methyl cellulose acetate succinate (HPMCAS AQOAT-MF) was from Shin-Etsu (Tokyo, Japan). The structures of IND, INDester, RTV, LOR, CLO, CIL, CNZ and HPMCAS are shown in Figure 1. Methanol (MeOH), dichloromethane (DCM), acetonitrile (ACN), tetrahydrofuran (THF), phenol, sulfuric acid, formic acid (FA), sodium hydroxide (NaOH), sodium chloride (NaCl), triethylamine (TEA), sodium phosphate dibasic anhydrous (Na_2HPO_4), and sodium phosphate monobasic monohydrate ($NaH_2PO_4.H_2O$) were purchased from Fisher Chemicals (Fair Lawn, NJ, USA). Glycine was purchased from Mallinckrodt Baker Inc. (Kentucky, USA). The composition of various buffer solutions is summarized in Table S1.

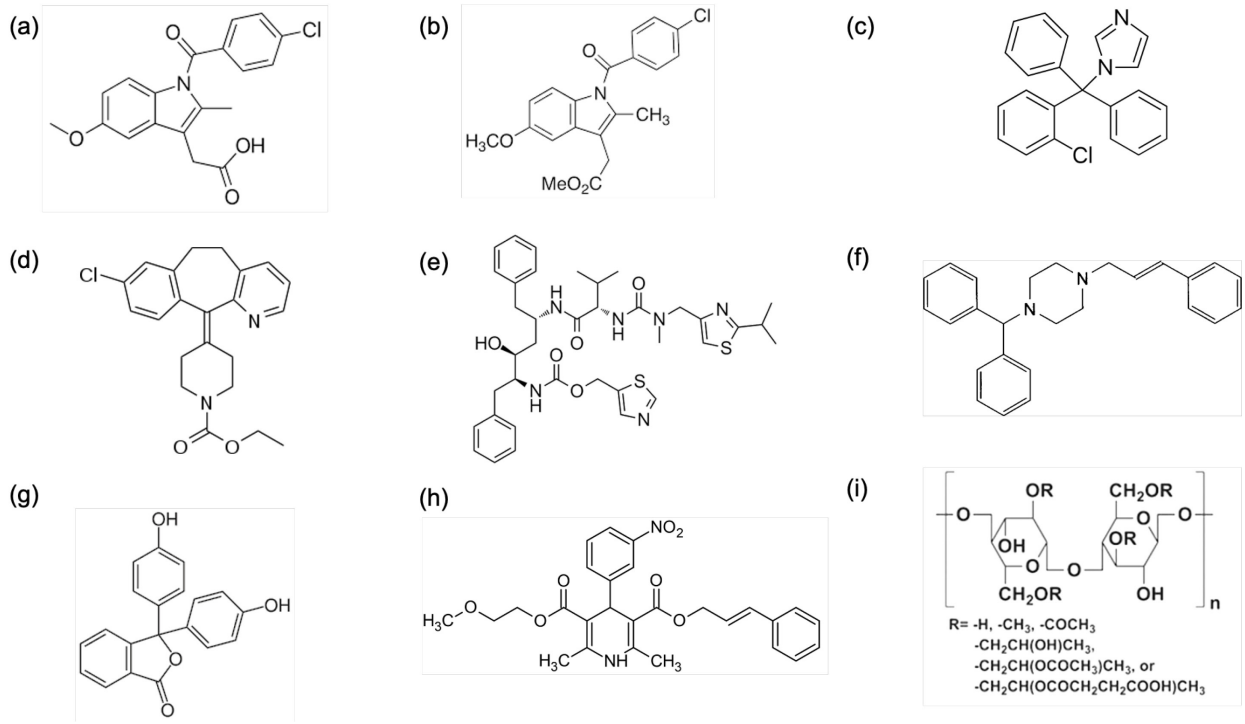

Figure 1. Structures of (a) indomethacin (IND), (b) indomethacin methyl ester (INDester) (c) clotrimazole (CLO), (d) loratadine (LOR), (e) ritonavir (RTV), (f) cinnarizine (CNZ), (g) phenolphthalein (PHPH), (h) cilnidipine (CIL), (i) hydroxypropyl methyl cellulose acetate succinate (HPMCAS).

3. Methods

3.1. Solubility

3.1.1. Crystal solubility

Solubility of crystalline drugs was determined after solid-solution equilibration. Briefly, an excess amount of crystalline drug was added to 15 mL buffer (pH 6.8, 7.5 or 9.0) in a jacketed beaker maintained at 37 °C. The suspension was stirred for 48 hours followed by ultracentrifugation in an Optimal-100 XP centrifuge (Beckman Coulter Inc., Brea CA) equipped with swinging bucket rotor SW 41 Ti at 35000 rpm for 30 minutes, 37 °C to separate the dissolved drug from undissolved particles. The concentration of the dissolved drug was

determined by reverse phase high performance liquid chromatography (HPLC) using an Ascentis® Express (Sigma-Aldrich, St. Louis, MO) 90 Å C18 column with dimensions of 15 cm × 4.6 mm and particle size of 5 µm. The details of the HPLC quantification methods for all model drugs are described in Table S2. The standard curves for all model drugs were prepared in triplicate in the concentration range of 0.1- 50 µg/mL with R^2 of 0.999.

3.1.2. Amorphous solubility

Amorphous solubility of LOR and CLO in buffers of different pH (pH 6.8, 7.5 and 9.0) was determined by the ultraviolet (UV) extinction method. Briefly, 5 mg/mL stock solution of the drug in THF was added to the buffer in a jacketed beaker maintained at 37 °C using a KD Scientific Legato 200 Syringe Pump (Holliston, MA) at 50 µL/min for LOR and 10 µL/min for CLO. The UV extinction was observed using a SI Photonic UV spectrophotometer (Tucson, Arizona) at 450 nm (a non-absorbing wavelength). The concentration at which scattering appeared was considered as the amorphous solubility.

3.2. Preparation of Amorphous Solid Dispersions

HPMCAS-based amorphous solid dispersions of drugs were prepared by rotary evaporation using a rotary evaporator (Hei-VAP Core rotary evaporator, Heidolph Instruments, Schwabach, Germany) equipped with an Ecodyst EcoChyll S cooler (Ecodyst, Apex, NC, USA). For indomethacin, various drug loadings (DL) of IND: HPMCAS ranging from 5% to 60% w/w were prepared by dissolving IND and HPMCAS in 1:2 v/v methanol: dichloromethane followed by rotary evaporation to remove the solvent with water bath maintained at 60 °C. For INDester, DLs ranging from 5%-60% w/w were prepared by dissolving INDester and HPMCAS in THF followed by rotary evaporation with the water bath maintained at 45 °C. For LOR, RTV, CNZ,

PHPH and CLO, HPMCAS-based ASDs of various drug loadings were prepared by dissolving drug and polymer in 1:2 v/v methanol: dichloromethane followed by rotary evaporation at 50 °C. Following rotary evaporation, ASDs were dried under vacuum overnight, and then cryomilled using a 6750 Freezer/Mill (SPEX SamplePrep, Metuchen, NJ) followed by sieving, retaining the particle size fraction, 106-250 μm. The amorphous nature of the ASDs was confirmed with powder X-ray diffraction (PXRD) and polarized light microscopy (PLM).

3.3. Preparation of Amorphous Drugs

Neat amorphous LOR, RTV and CNZ were prepared by melt quenching. 2 g of each drug was heated to 10 °C above the melting point in an oven, rapidly cooled with liquid nitrogen and cryomilled. The amorphous nature was confirmed with polarized light microscopy (PLM).

3.4. Analysis of Polymer Concentration

3.4.1. HPLC analysis

The concentration of HPMCAS following ASD dissolution was analyzed by HPLC using a Shodex RS pak DS-413 column. A gradient method was developed, and polymer was detected using an evaporative light scattering detector (ELSD). The mobile phases consisted of 0.1% formic acid in water and 0.1% formic acid in acetonitrile, the injection volume was 80 μL and the flow rate was 0.5 mL/min. A continuous flow of high-pressure liquid nitrogen at a rate of 1.5 standard L/min minute was required for the ELSD detector. The nebulizer temperature was maintained at 80 ºC and the evaporator temperature was maintained at 85 ºC. Standard curves were prepared in triplicate in the concentration range of 1-250 μg/mL with an R^2 of 0.999.

3.4.2. Colorimetric analysis

HPMCAS in the supernatant was also analyzed by colorimetric analysis for the complexation experiments using a Varian Cary 300 Bio (Varian, Inc., Palo Alto, CA, USA) UV-visible

spectrophotometer. Briefly 10 µL of phenol solution (4 g in 1 mL of ultrapure water) was added to 400 µL of sample and vortexed for 5 s. Next, 1 mL of sulfuric acid was added, and samples were left for 1 h for color development, followed by measurement of the absorbance at 490 nm. Standard curves were prepared for the concentration range of 1-100 µg/mL with R^2 of 0.999.

3.5. Surface Area Normalized Dissolution

An intrinsic dissolution rate (IDR) Wood's apparatus (Agilent Technologies, Santa Clara, CA) was used to perform surface area normalized dissolution experiments on neat amorphous drug, neat polymer and ASDs whereby only one surface of the compact was exposed to buffer solution in a jacketed beaker maintained at 37 ºC. Briefly, 100 mg of the sample was weighed and compressed in an 8 mm die (surface area of 0.5 cm^2) using a Carver press (Carver, Wabash, IN) at 1500 psi for one minute. The die was then attached to a spindle rotating at 100 rpm and immersed in a water bath containing buffer maintained at 37 °C. The dissolution experiment was performed for 1 hour with samples taken at 5, 10, 15, 20, 25, 30, 40 and 60 minutes. The sampled volume was replenished with fresh buffer. The samples were then analyzed by HPLC for drug and polymer using the aforementioned methods. The normalized release rate of the drug and polymer is calculated from equation 1.

$$R = \frac{k \times V}{S \times x} \qquad \text{(eq. 1)}$$

where k is the slope of the regression line, V is the volume of dissolution medium (100 mL), S is the surface area of the die exposed to the dissolution medium (0.5 cm^2) and x is the weight fraction of each component.

3.6. X-ray Photoelectron Spectroscopy (XPS)

Reference compacts of neat CNZ, neat HPMCAS and sample compacts of 25% DL CNZ: HPMCAS-based ASDs before and after partial dissolution were manually ejected. These

compacts were dried overnight under vacuum, and their surface composition was analyzed using XPS. A Kratos Axis Ultra DLD spectrophotometer (Kratos Analytical Inc., Manchester, UK) was used to obtain XPS data using monochromatic A1 K*a* radiation (1486.6 eV) at constant pass energy (PE) of 20 and 160 eV for high-resolution and survey spectra acquisition, respectively. A commercial Kratos charge neutralizer was used to neutralize the surface charge of the non-conducting tablet surface during data acquisition and to obtain better resolution. The instrument resolution for a PE of 20 eV is about 0.35 eV. Binding energy (BE) values refer to the Fermi level and the BE scale was calibrated using Au $4f_{7/2}$ = 84.0 eV and Cu $2p_{3/2}$ = 932.67 eV. Compacts were placed on a stainless-steel sample holder bar using a double-sided sticking Cu tape with the surface of interest facing upwards. *CasaXPS* software was used to analyze the XPS data. The charge correction was applied prior to data analysis by setting the C-C component of the C 1s peak at BE of 284.8 eV. The atomic concentrations of the elements in the near-surface region (~ 10 nm) was estimated after Shirley or Tougaard background subtraction. Curve fitting was performed using Gaussian/Lorentzian peak shape (the protonated N 1s component) and the peak obtained from the reference compound (the N 1s peak of cinnarizine). 3-5 spots were measured on each sample. The N 1s peaks of neat CNZ, CNZ: HPMCAS 25% DL before and after partial dissolution (40-45 minutes) were analyzed and compared to determine the relative percentage protonation.

3.7. Drug-Polymer Complexation

Drug-polymer insoluble complex formation was evaluated to determine the extent of interaction between the drug and polymer. Three sets of stock solutions were prepared in THF, one containing neat drug, the second containing neat polymer at a concentration of 52.5 mg/mL and the third containing defined stoichiometric ratios of drug and polymer (polymer concentration

was fixed as 52.5 mg/mL), calculated as number of moles of drug per mole of HPMCAS succinoyl groups, where the molar substitution of HPMCAS-MF with respect to succinoyl groups has been reported previously.[14]

As an initial control experiment, neat drug was added to the medium. When a small aliquot of a concentrated stock solution of neat CNZ was added to agitated pH 6.0 50 mM phosphate buffer to create a concentration of 460 µg/mL, the solution became turbid. After centrifugation, the pellet was assayed, and consisted of drug. In contrast, when a small aliquot of concentrated stock solution of neat HPMCAS was added to pH 6.0 50 mM phosphate buffer to create concentration of 1 mg/mL, it completely dissolved and resulted in clear buffer solution, where no pellet was formed following centrifugation. When CNZ and HPMCAS were coadded to pH 6.0 50 mM phosphate buffer, a precipitate was observed that could be pelleted by ultracentrifugation. This precipitate was then analyzed by HPLC or colorimetry to determine the presence and amount of HPMCAS. Given that HPMCAS is soluble in the buffer at this pH, its presence in the precipitate indicates formation of an insoluble complex with the drug. The precipitate was confirmed to be amorphous using PLM. Next, a series of drugs were evaluated at select drug: polymer ratios and at pH 6.0. The percent of polymer complexed was determined using the following equation:

$$\%\ Polymer\ complexed = \left(1 - \frac{Polymer\ in\ the\ supernatant}{Total\ polymer\ in\ the\ solution}\right) \times 100 \qquad \text{(eq. 2)}$$

The final concentration of organic solvent in the buffer was 10-20 µL/mL. The final polymer concentration in the buffer ranged between 0.5-1.0 mg/mL, far below its solubility of 5 mg/mL at pH 6.[47] Unless otherwise noted, the complexation studies were performed at pH 6.0 in order to mimic the pH at the HPMCAS gel layer-bulk solution interface. The pH at the gel-solution interface is lower than the bulk solution pH due to the release of protons following HPMCAS ionization, and for a 50 mM pH 6.8 phosphate buffer system the gel layer has been estimated as

pH 6.0[46] and is therefore the relevant pH to evaluate possible complexation in terms of its impact on release rate. Selected complexation studies were also performed at other pH values in the case of LOR in order to study the impact of drug ionization extent on complexation.

4. Results

4.1. Solubility

The equilibrium solubilities of crystalline and amorphous model drugs are summarized in Table 1.

Table 1. Crystal and amorphous solubilities of model drugs at various pH conditions. Mean values ± standard deviation where n=3. Some values were taken from the literature and the reference is given as a superscript.

	pH	IND	INDester	RTV	LOR	CLO	CNZ	PHPH	CIL
Crystal solubility (µg/mL)	6.8	459 ± 10[46]	0.6 ± 0.1[46]	1.3 ± 0.2[48]	1.8 ± 0.1	0.80 ± 0.06	2.1 ± 0.06[49]	ND	0.05 ± 0.0[16]
	7.5				1.4 ± 0.1				
	9.0					0.40 ± 0.02			
Amorphous solubility (µg/mL)	6.8		3.8 ± 0.4[46]	18.8 ± 0.07[48]	9.0 ± 0.1	9.00 ± 0.06	12.0 ± 0.2[50]	200 ± 20[18]	0.6 ± 0.1[16]
	7.5				7.6 ± 0.1				
	9.0					5.2 ± 0.1			

4.2. Surface Area Normalized Dissolution

4.2.1. Weakly Acidic (WA) and Neutral Drugs

Figure 2 shows normalized release rates of HPMCAS-based ASDs of IND, a weakly acidic drug with a pK_a of 4.5,[51] at various drug loadings in 50 mM pH 6.8 phosphate buffer. Drug and polymer release at similar normalized release rates indicates that the release was controlled by the polymer. A similar plot for INDester-HPMCAS ASDs is shown in Figure 3. Both ASDs showed a decreased

polymer release rate in comparison to the neat polymer, where the polymer release rate became slower with increasing drug loadings. From a comparison of the data in Figures 2 and 3, it is apparent that IND showed a higher normalized release rate compared to INDester when comparing equivalent drug loadings and thus had less impact on the release rate of HPMCAS. Release rate data for PHPH at a single drug loading is summarized in the Table S3.

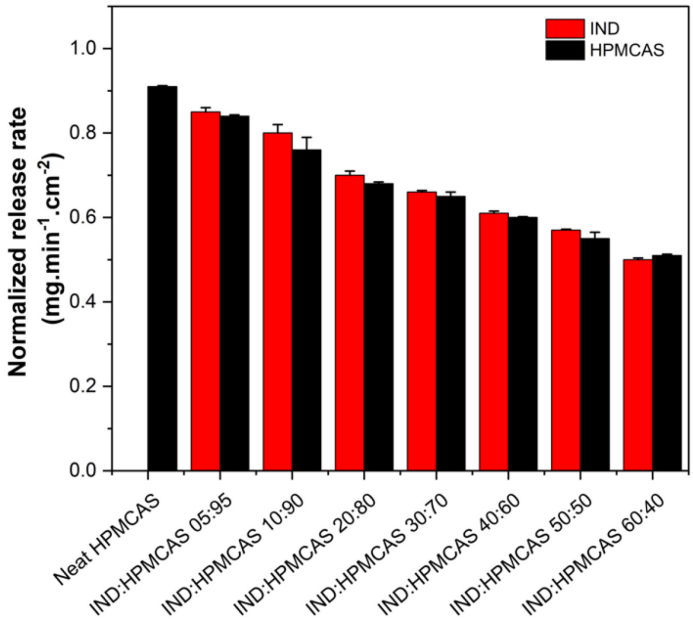

Figure 2. Normalized release rates of various drug loadings of IND: HPMCAS ASDs. Error bars represent standard deviations, n = 3. 10 and 50% DL results are taken from Bapat et al.[46]

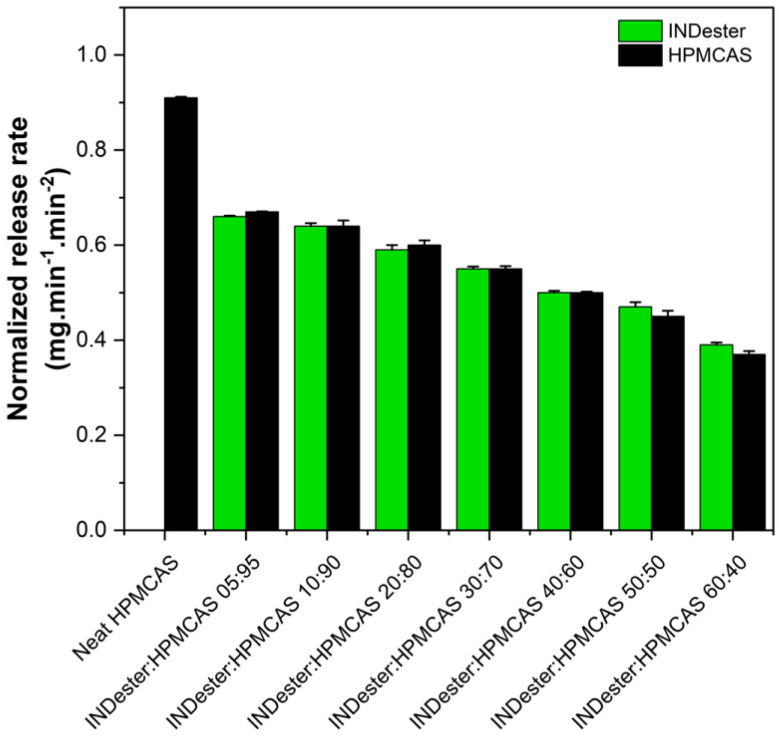

Figure 3. Normalized release rates of various drug loadings of INDester: HPMCAS ASDs. Error bars represent standard deviations, n = 3. 10 and 50% DL results are taken from Bapat et al.[46]

4.2.2. Weakly Basic Drugs (WB)

Weakly basic drugs were classified into three categories based on the extent of ionization at a dissolution pH of 6.8. Table 2 summarizes the three categories along with the pK_a's.

Table 2. Classification of weakly basic drugs based on extent of ionization and literature pK_a values

Predominantly unionized	Partially ionized		Predominantly ionized
Ritonavir (RTV) $pK_a = 2.6$[52]	Loratadine (LOR) $pK_a = 5.2$[53]	Clotrimazole (CLO) $pK_a = 5.9$[53]	Cinnarizine (CNZ) $pK_a = 8.4$[54]

The normalized release rates of 25% DL ASDs of RTV, LOR, CLO and CNZ are shown in Figure 4, and release rates for select ASDs of different drug loadings are summarized in Table S3

The surface area normalized dissolution experiments for WB ASDs were performed at two pH

values for LOR and CLO, one where the drug is partially ionized and one where it is predominantly unionized, to assess the impact of ionization extent. For RTV: HPMCAS ASD, the surface area normalized dissolution experiment was performed only at pH 6.8 where RTV is predominantly unionized. Experiments couldn't be performed at a pH where this compound is ionized (< pH 2) since HPMCAS is insoluble at low pH. For CNZ, given its relatively high pK_a, this compound is predominantly ionized at all physiologically relevant pH values. For LOR: HPMCAS ASD, the dissolution experiment was performed at pH 6.8 where LOR is partially ionized and at pH 7.5 where LOR is predominantly unionized. Similarly, for CLO: HPMCAS ASD, the dissolution experiment was performed at pH 6.8 (partial ionization) and at pH 9.0 (predominantly unionized). The lower release of neat polymer in pH 9.0 glycine: NaOH buffer corresponded to its lower buffer capacity at the dissolving interface compared to the bulk solution showing the impact of pK_a of buffer (pK_a = 9.0) with respect to surface pH (the tablet didn't form a gel layer when dissolving in 50 mM pH 9.0 glycine: NaOH buffer indicating the surface pH was lower than 5.5) .

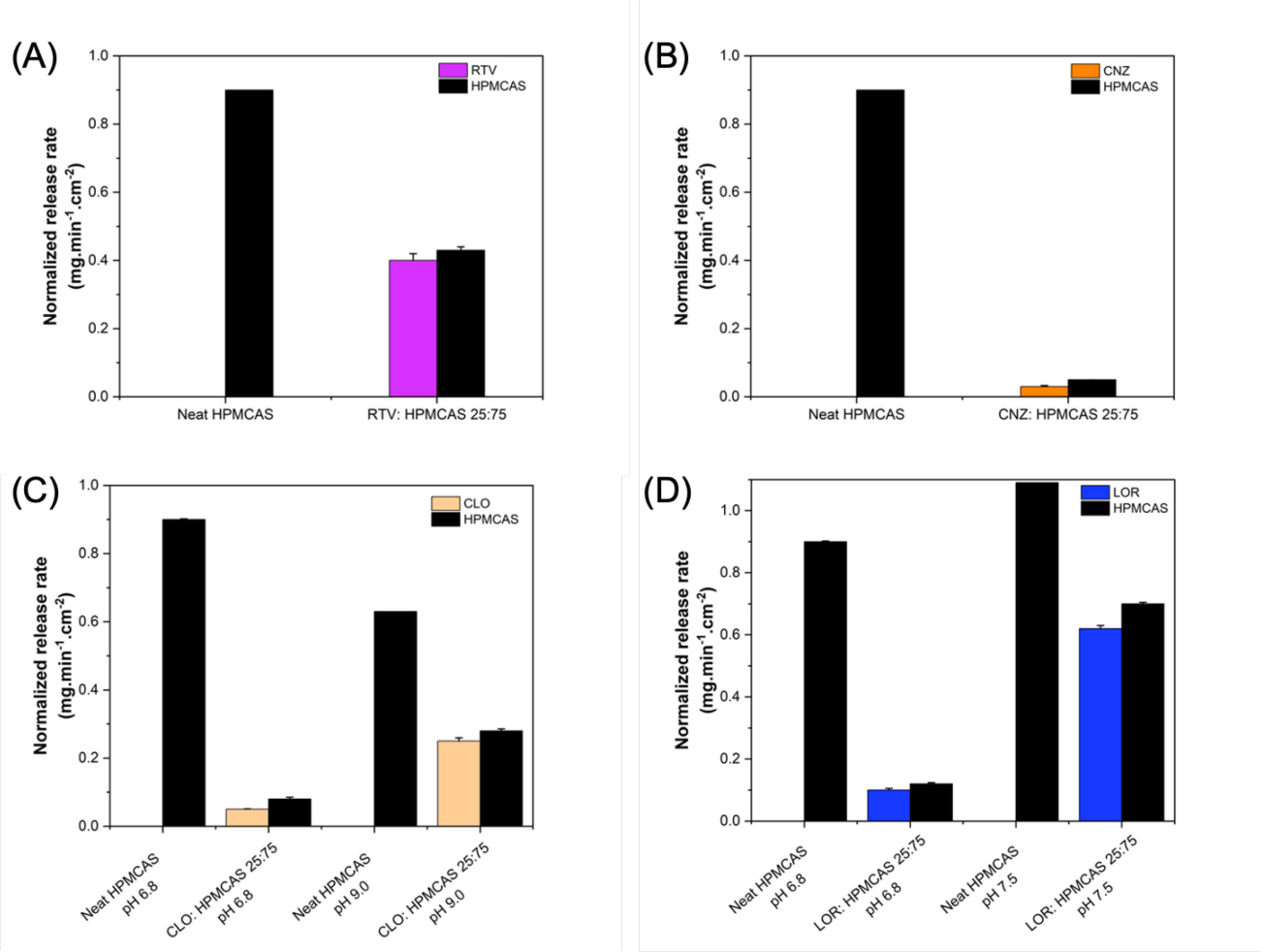

Figure 4. Normalized release rates of components from neat HPMCAS and 25% DL ASDs of (A) RTV: HPMCAS at pH 6.8, (B) CNZ: HPMCAS at pH 6.8, (C) CLO: HPMCAS at various pH values, (D) LOR: HPMCAS at various pH values. Error bars represent standard deviations, n = 3.

For all ASDs of HPMCAS with a weakly basic drug, the release rate of the polymer decreased as compared to the neat polymer. The ratio of neat HPMCAS release rate to that from the ASD is summarized in Figure 5 for the different systems. The largest retardation in polymer release rate (highest ratio) at pH 6.8 was observed in the presence of CNZ, which is predominantly ionized, where the neat polymer had a 30-fold higher dissolution rate than the polymer in the ASD. The next largest impact was seen for LOR and CLO at a pH where they were partially ionized, while

the lowest impact was observed for RTV. Increasing the pH to decrease the ionization extent of LOR and CLO reduced their deleterious impact on HPMCAS release.

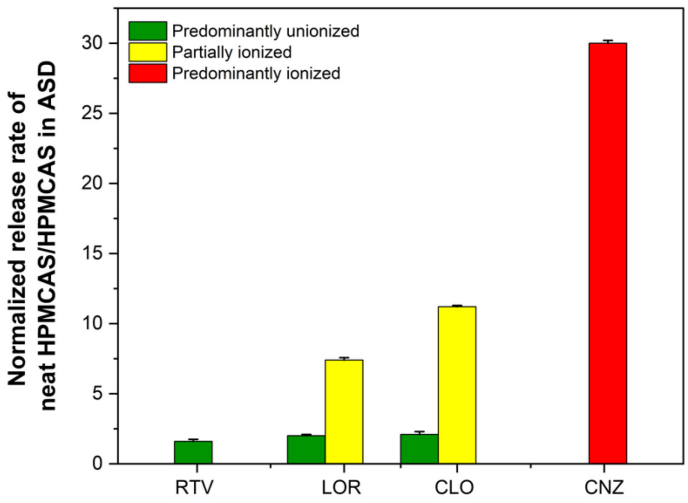

Figure 5. Ratio of the normalized release rate of neat HPMCAS: HPMCAS in the ASD at a pH where drug is predominantly unionized, partially ionized, or predominantly ionized. Error bars represent standard deviations, n = 3.

To study the impact of ionic strength, the surface area normalized release rates for neat HPMCAS and the corresponding 25% DL ASD with LOR were compared in 50 mM and 100 mM pH 6.8 phosphate buffer (Figure 6). Increasing the buffer salt concentration from 50 mM to 100 mM improved release of both components from the ASD (factor of ~2.9 improvement) to a much larger extent than the increase observed for the neat HPMCAS which was minimal (factor of ~1.2 increase).

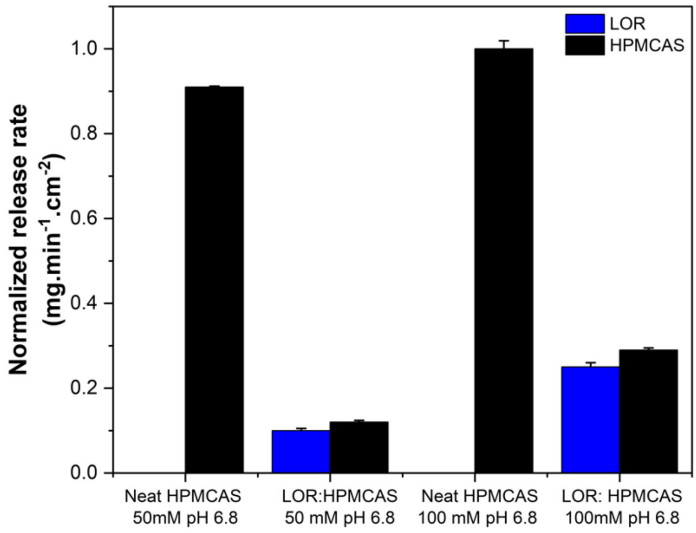

Figure 6. Normalized release rates of neat HPMCAS and 25% DL of LOR: HPMCAS at 50 mM and 100 mM pH 6.8 phosphate buffer. Error bars represent standard deviations, n = 3.

Surface area normalized dissolution experiments for neat amorphous LOR were also performed at pH 3.0, pH 6.8 and pH 7.5. As shown in Figure 7, amorphous LOR had a higher normalized release rate in media where the drug was ionized (pH 3.0) as compared to when it was unionized (pH 7.5).

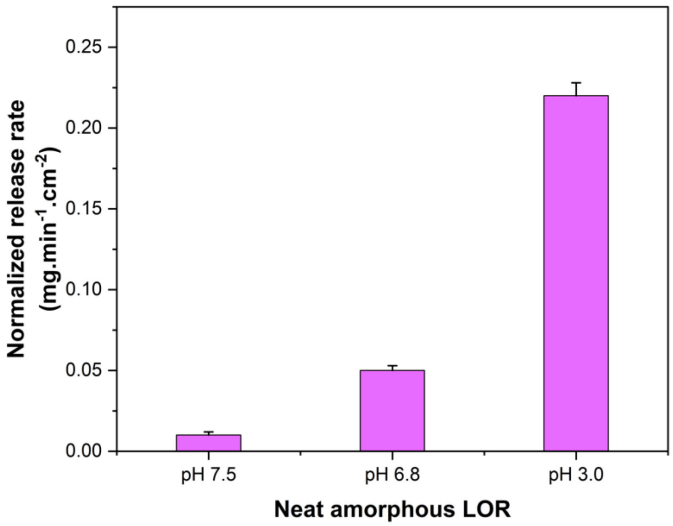

Figure 7. Normalized release rate of neat amorphous loratadine at pH 7.5, 6.8 and 3.0. Error bars represent standard deviations, n = 3.

4.3. X-ray Photoelectron Spectroscopy (XPS)

Figure 8 shows the N 1s peak of neat amorphous CNZ, and the corresponding peak for a 25% DL CNZ: HPMCAS ASD before and after a partial dissolution of a compact. No protonation was observed in case of the neat CNZ (Figure 8A). However, a shift in the peak shows some extent of protonation of the N 1s peak of the CNZ: HPMCAS ASD before dissolution (Figure 8B), which persisted after partial dissolution (Figure 8C). The decrease in % protonation after partial dissolution is consistent with the observed surface drug enrichment relative to the polymer. The percent protonation for each sample, calculated by peak fitting (green curves in Figure 8B, C) is listed in Table 3.

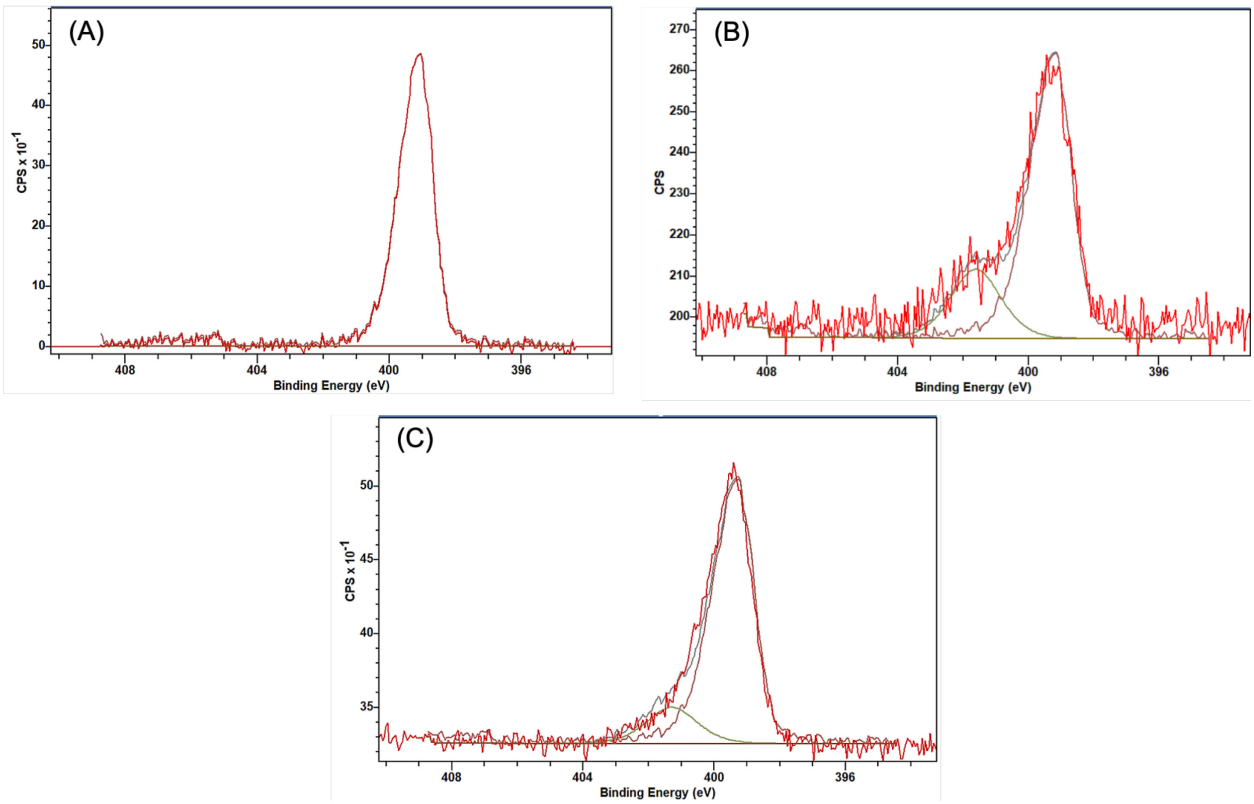

Figure 8. N 1s spectrum of (A) Neat CNZ, (B) 25% DL CNZ: HPMCAS-MF (before dissolution), (C) 25% DL CNZ: HPMCAS-MF (after partial dissolution at pH 6.8)

Table 3. Percent protonation calculated from N 1s spectra of neat CNZ, 25% DL CNZ: HPMCAS-MF before and after dissolution. Mean values ± standard deviation where n=3.

N 1s spectrum	% protonation
Neat CNZ	0 ± 0
CNZ: HPMCAS-MF (before dissolution)	20 ± 1
CNZ: HPMCAS-MF (after dissolution)	11 ± 1

4.4. Analysis of Drug and Polymer in Precipitates

Precipitates were quantitively analyzed to determine the relative amounts of drug and polymer. Figure 9 shows the percent polymer complexed with ionized CNZ in the precipitate for various molar ratios of CNZ: COOH content of HPMCAS in pH 6.0 phosphate buffer.

The polymer-drug complexation increased as molar ratio of drug: polymer COOH groups was increased, whereby >90% of the HPMCAS was in the form of an insoluble precipitate at a 1:1 molar ratio and at a 2:1 molar ratio, ~100% of the polymer formed an insoluble complex with the drug. A 1:1 molar ratio of CNZ: COOH content of HPMCAS, corresponds to a ~30% DL ASD. A lower ratio of 0.25: 1 CNZ: COOH groups (corresponding to 10% DL CNZ: HPMCAS ASD) showed less complexation (~40%).

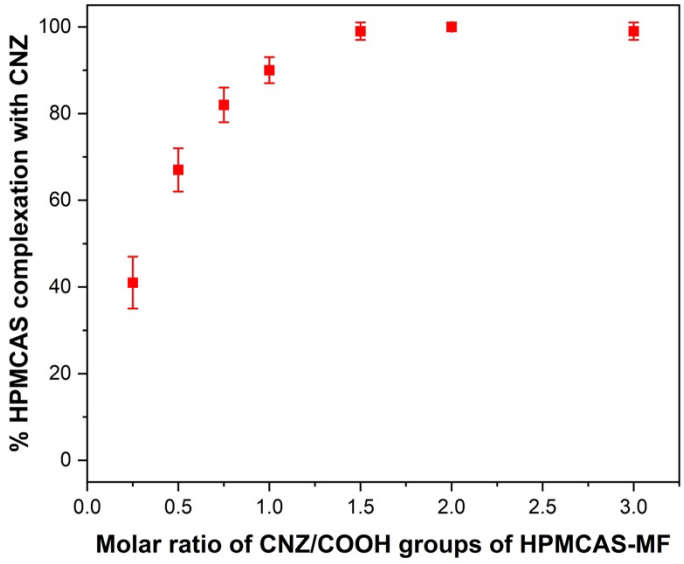

Figure 9. HPMCAS complexation with CNZ at various molar ratios of CNZ to COOH groups of HPMCAS-MF at pH 6.0. Error bars represent standard deviations, n = 3.

Table 4. Impact of drug on the extent of HPMCAS-MF complexation at different drug: polymer COOH groups molar ratios. Mean values ± standard deviation where n=3.

Drug	Drug:polymer molar ratio	Corresponding ASD Drug loading (%)	Polymer Complexation (%)
Indomethacin (IND)	1:1	30	5 ± 2
	2:1	60	8 ± 2

Indomethacin methyl ester (INDester)	1:1	30	7 ± 2
Ritonavir (RTV)	0.1:1	10	6 ± 1
	0.4:1	25	11 ± 2
	1:1	47	15 ± 3
Cilnidipine (CIL)	1:1	40	17 ± 3
Loratadine (LOR)	0.25:1	10	30 ± 5
	0.55:1	20	47 ± 4
	0.75:1	25	63 ± 2
	1:1	30	70 ± 5
Phenolphthalein (PHPH)	1:1	27	60 ± 4
Clotrimazole (CLO)	0.8:1	25	80 ± 3
Cinnarizine (CNZ)	0.125:1	5	12 ± 3
	0.25:1	10	40 ± 6
	0.75:1	25	83 ± 4
	1:1	30	90 ± 5

For the unionized drugs, RTV, CIL and INDester, and the negatively charged IND, only ~5-17 % of the polymer formed an insoluble complex with the drug for a 1:1 molar ratio. The ionized/partially ionized cationic drugs (LOR, CNZ and CLO) led to a much higher extent of insoluble complex formation, ≥70% for a 1:1 ratio. Interestingly, the unionized compound, PHPH, also underwent a high extent of complexation with HPMCAS.

For LOR, the extent of complexation over the pH range of 5.8-6.5 was monitored, whereby the change in the extent of drug ionization is expected to be notable based on a reported pK_a value of 5.2.[53] Consistent with the importance of the ionization state of the drug, the complexation curve for a 1: 1 molar ratio of LOR:COOH groups shows a steep dependence on bulk solution pH. As the pH decreased from pH 7.5 to pH 5.8, the extent of complexation increased. This is consistent with a stronger interaction between the cationic form of LOR with the with anionic groups of HPMCAS relative to the interaction between polymer and unionized drug. The steepness of % complexation curve with pH is also consistent with the expected dependence of the ionization reaction with pH, although it is not perfectly predicted based on the reported drug pK_a. This is

not unreasonable given that pK_a values are known to vary depending on the local microenvironment.[55,56]

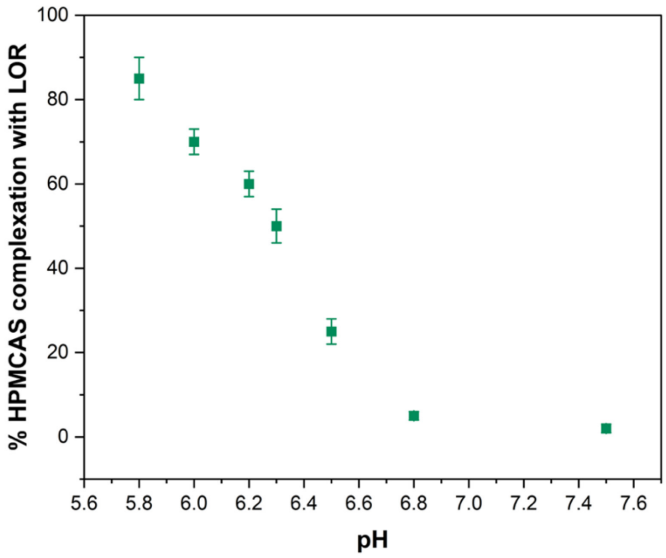

Figure 10. Percentage HPMCAS complexation with LOR at various pH values for 1:1 molar ratio of LOR: COOH groups of HPMCAS. Error bars represent standard deviations, n = 3.

5. Discussion

Recent studies suggest a correlation between drug-polymer interactions and ASD release performance for copovidone-based ASDs containing lipophilic drugs whereby drug-polymer hydrogen bonding interactions led to poor release performance at even modest drug loadings.[17,18,23] For HPMCAS or other enteric polymers, the impact of drug-polymer interactions is largely unknown, and, for these specific polymers, it is also important to consider the potential impact of drug-polymer ionic interactions. When considering how drug-polymer interactions can impact polymer release, and consequently drug release (since drug and polymer release appear co-dependent for the HPMCAS ASDs studied herein, e.g. see Figure 4), it is relevant to briefly discuss how glassy polymers dissolve. Following water ingress into the matrix (i.e. hydration), plasticization occurs, increasing molecular mobility and ultimately leading to diffusion of the hydrated polymer chains into bulk solution if the solvent quality is sufficiently high for polymer solubility. For HPMCAS, the protonated polymer interacts to a low extent with water, thus a critical extent of ionization is required for the polymer chains to become sufficiently hydrated to solubilize, and hence a threshold pH is required before dissolution occurs. Furthermore, addition of a lipophilic drug to a polymer to form an ASD reduces the rate and overall extent of hydration, since the drug has a much lower affinity for water than the polymer. Consequently, increasing the ASD drug loading is expected to delay the release of ASDs components since the polymer dissolution rate will be reduced, as illustrated in Figures 2-3. However, if drug lipophilicity was the only factor involved in reducing polymer hydration, then drugs of similar lipophilicity should yield similar relationships between release rate and drug loading. Figure 11 shows a comparison of release rate versus drug loading (taken from Table S3) for several of the lipophilic drugs studied herein which have somewhat comparable Log P values. It is clear that some drugs are

more effective at delaying release of components from an ASD than others. Notably, CNZ, which is cationic at pH 6.8 is the most detrimental to release, while IND (anionic) and INDester (unionized) have lower impact. These observations strongly suggests that drug-polymer interactions play a critical role in HPMCAS-based ASD dissolution, in addition to drug lipophilicity.

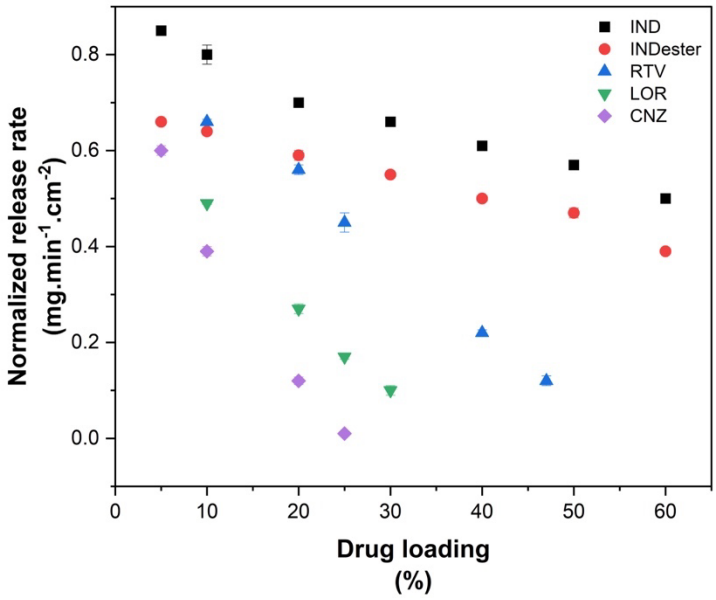

Figure 11. Drug release rates of various HPMCAS-based ASDs as a function of drug loading at pH 6.8. Error bars represent standard deviations, n = 3. Log P values are 4.1 (IND), 4.5 (INDester), 5.7 (RTV), 4.55*(LOR), 5.9* (CNZ). *Values calculated from Chemaxon software, version 23.5.0.

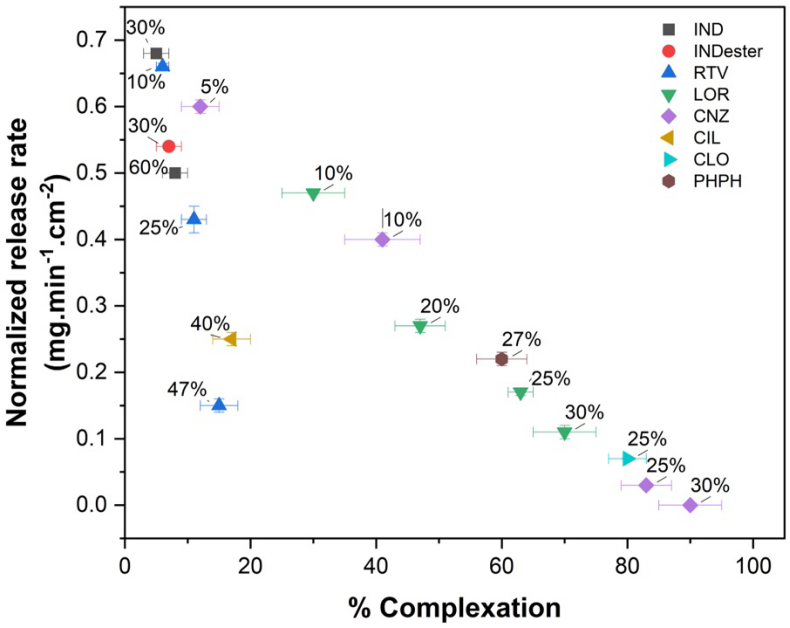

Figure 12. Relationship between normalized release rates of drug, % complexation and drug loading for HPMCAS ASDs with various drugs. The numerical notation by each symbol indicates the drug loading at which the drug release rate was measured, and the extent of insoluble complex formation was determined at the corresponding polymer: drug ratio. Error bars represent standard deviations, n = 3.

Figure 12 provides insight into the relationship between insoluble complex formation and ASD release properties. The drugs studied fall roughly onto two trendlines when the relationship between the normalized release rate of the drug from the ASD and the percentage of insoluble drug-polymer complexation for a comparable drug: polymer ratio is examined. Drugs that had a low extent of complexation with HPMCAS, even for higher drug: polymer ratios (corresponding to a higher drug loading), fall on the left side of the plot. These drugs are anionic (IND) or unionized (CIL, INDester, RTV) at the dissolution pH. For these drugs, the diminished release rate can likely be attributed mainly to the drug lipophilicity, where reduced release rates are observed for higher drug loading ASDs because of a lower extent of hydration. These drugs are expected to interact weakly with ionized HPMCAS based on their chemistry, although it is

interesting that some extent of insoluble complex formation is observed, in particular as the drug: polymer ratio is increased. In contrast, LOR, CNZ, CLO and PHPH lie on a second trendline to the right of the plot. Drugs in this region of the plot had high extents of complexation with the polymer at pH 6.0 and exhibited greatly reduced release rates at even lower drug loadings.

HPMCAS has a solubility of approximately 5 mg/mL at pH 6.0,[47] resulting from extensive ionization. In the presence of certain lipophilic drugs, the polymer solubility was reduced at this pH due to drug-polymer complexation which led to precipitation. The link between drug-polymer insoluble complexation formation and the reduced release rates can be rationalized by considering the rate controlling step for dissolution of HPMCAS-based ASDs. Previous studies have shown the drug release rate from HPMCAS-based dispersions depends on polymer release rate.[3,11,14,28,46] Thus, if a molecularly dispersed drug results in a decrease in the polymer release rate, the drug release rate is, in turn, reduced. We recently postulated based on experimental observations that the rate limiting step for HPMCAS dissolution is the polymer solubility at the gel-solution interface, which in turn impacts the polymer diffusivity as shown by equation 3.

$$J_p = \frac{D_p}{\delta} C_p \qquad \text{(eq. 3)}$$

Where J_p is the polymer flux, D_p is the polymer diffusion coefficient, C_p is polymer solubility at the polymer-solution interface, and δ is the thickness of the boundary layer. HPMCAS solubility is a strong function of pH, and we have shown a relationship between the neat polymer release rate and the pH at the gel-solution interface, as well as other studies that suggest that equation 3 explains HPMCAS dissolution behavior.[46] Consequently, any factors that impact the polymer solubility i.e. insoluble complex formation with a drug are expected to alter polymer dissolution.

Because drug-polymer interactions modulate HPMCAS solubility, equation 3 can be used to partially rationalize the reduced release rates as a function of complexation noted in Figure 12, with a reduced rate of hydration due to drug lipophilicity likely also contributing. Reduced solubility due to complexation likely largely accounts for the systems falling on the righthand side trend line in Figure 12, while lipophilicity is likely the dominant factor for systems falling on the left-most trendline.

It is well known that the aqueous solubility of a molecule can be reduced through complex formation with an oppositely charged, amphiphilic molecule.[57] Such complexes are often called hydrophobic ion pairs, whereby this phenomenon has been widely observed for charged proteins, peptides and small molecule drugs paired with amphiphiles such as surfactants.[58–62] Further, the complexation of an ionic polymer, which is a polyelectrolyte, with an oppositely charged amphiphilic molecule to form an insoluble complex has been widely studied.[63–65] Thus, the anionic surfactant, sodium dodecyl sulfate, led to the precipitation of a cationic cellulose polymer.[66] In addition to surfactants, polyelectrolyte precipitation has been observed for anionic polymers such as dextran sulfate or alginate, and amphiphilic, cationic drugs including ciprofloxacin,[63] chlorpromazine, amitriptyline and doxepin.[67] Finally, we note that ion pairing between two oppositely charged polyelectrolytes with precipitation is a widely observed phenomenon typically referred to as complex coacervation.[68–70]

It is generally recognized that (in aqueous media) there are two contributing forces to the binding between oppositely charged polymers and amphiphiles (which ultimately leads to precipitation), namely electrostatic attraction and hydrophobic interactions.[71] Sundelöf and coworkers have performed extensive studies investigating factors that impact the binding of a positively charged, amphiphilic drug, to a negatively charged polysaccharide. They noted that the following factors

impact the binding: 1) drug hydrophobicity; 2) polymer charge density; 3) polymer chain flexibility. In addition, pH, ionic strength, and the type of ions present will affect the interactions. For the complexation studies conducted herein at pH 6.0, HPMCAS was approximately 96 % ionized (assuming a pK_a value of 4.9[14]). CNZ was >99 % ionized at this pH, while LOR and CLO were 14 and 46 % ionized, respectively, based on the pK_a values listed in Table 2. For the CNZ-HPMCAS system, both species were thus nearly completely ionized in the hydrated gel layer. The ionization largely occurs upon hydration within the gel layer, given the observation from XPS (Figure 8 and Table 3) that only approximately 25% of CNZ is ionized in the dry ASD. Further, a plateau in complexation was observed at a molar ratio of approximately 1.5 moles drug: polymer COOH groups. An excess of drug cations beyond the expected 1:1 stoichiometric ratio typically observed for electrostatically driven complexation likely resulted because of the relatively high ionic strength of the medium (ionic strength = 63 mM) and the resultant shielding effect of the buffer ions leading to less efficient complex formation. Furthermore, given the high tendency for complexation, even in the presence of additional solution ions, it appears unlikely that the drug-HPMCAS insoluble complex would be disrupted at biologically relevant ionic strength conditions (also see Figure S1).

Moving to the partially ionized systems, LOR has a pK_a such that the role of drug ionization extent on the complexation can be evaluated, while maintaining HPMCAS in its ionized form. From Figure 10, it is clear that ionization of LOR is necessary for insoluble complexation with HPMCAS. Thus, at a pH >>pK_a, complexation was not observed, whereas as pH is decreased towards pK_a, the extent of complexation increased. It can be concluded that LOR, which lacks hydrogen bond donors, mainly interacts with ionized HPMCAS via electrostatic interactions. The high extent of complexation observed for a modest theoretical extent of ionization could

result either from an increased apparent pK_a of LOR when bound to the negatively charged HPMCAS,[72] or cooperatively in binding resulting from hydrophobic interactions.[73] The importance of considering the gel layer pH rather than the bulk solution pH is also highlighted by the LOR-HPMCAS system, as illustrated in Figure 13. While complexation is negligible at a bulk solution pH of 6.8, ASD release is substantially compromised at this pH. This can be attributed to the much lower gel layer pH,[46] where some extent of complexation is possible, leading to a reduced polymer dissolution rate. The steep dependence of release rate over the gel layer pH range of pH 6.0-6.3 (Figure 13) corresponds to a steep portion of the % complexation versus pH curve shown in Figure 10.

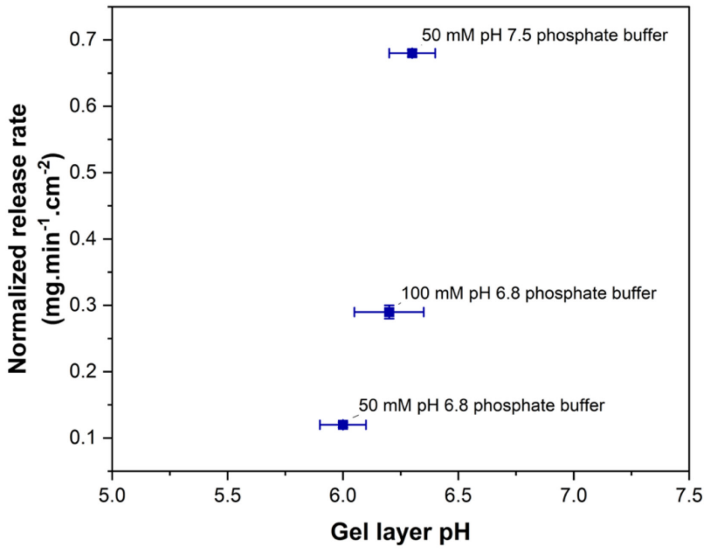

Figure 13. Normalized release rate of LOR: HPMCAS 25:75 at various gel layer pH. Error bars represent standard deviations, n = 3.

In addition to the cationic drugs, whose impact on HPMCAS solubility can be readily rationalized by considering electrostatic interactions with the resultant formation of a hydrophobic complex, we note that the neutral compound, PHPH, was quite efficient at forming a complex with HPMCAS, as well as reducing the drug release rate, falling on the same trend

line as the cationic drugs (Figure 12). This observation can be rationalized by considering the phenomenon of hydrophobic hydrogen bonding as described by Bernkop-Schnürch and co-workers.[74] They reported that the lipophilic complexes were formed via hydrogen bonding between a hydrophilic macromolecular drug and a non-ionic surfactant, observing > 50% precipitation efficiency of leuprolide at a pH less than its isoelectric point, in the presence of sucrose fatty acid esters. PHPH has been noted to form an insoluble complex with copovidone in aqueous solution, likely via hydrogen bond formation.[18] The carboxylate ion of HPMCAS provides a hydrogen bonding site for interaction with PHPH phenolic groups. In support of this conjecture, phenol has been observed to form hydrogen bonding complexes with various carboxylate ions (including succinate) in aqueous solution.[75]

Turning our attention to the other tested drugs, which had <20% complexation with the polymer, it is likely that the increased lipophilicity of the ASD plays a major role in the reduction in drug release rate with increasing drug load, as the presence of the drug will decrease the rate and extent of hydration of the ASD and hence the polymer. Still, it is interesting that for this group of drugs, the release still trends with the extent of complexation, where the drugs which tend to form more insoluble complex with the polymer show decreased release rates. From a practical perspective, much higher drug loadings can be achieved with these drugs before release rate impairment is observed, relative to the (predominantly) cationic drugs that more extensively complex with HPMCAS.

These observations have important implications for polymer choice when formulating an ASD. In summary, the chemistry, pK_a and Log P of the drug, as well as the buffer capacity, pH and ionic strength of the medium (via impact on gel/boundary layer pH), and drug loading are all likely determinants of the release rate of components from HPMCAS-based ASDs. Based on our

observations, weakly basic lipophilic drugs with pK_a's > 5 may lead to poor release from HPMCAS-MF ASDs, in particular at drugs loadings that exceed a 1:1 molar ratio of drug cations to polymer anionic groups.

6. Conclusions

When formulating ASDs with HPMCAS and a poorly water-soluble lipophilic drug, the chemistry of the drug should be considered in terms of its ability to form interactions with the polymer that can persist in an aqueous environment. These interactions are important for the release performance of the ASD, and are most relevant for lipophilic, weakly basic drugs that can form electrostatic interactions with HPMCAS when both species are mutually ionized. Such electrostatic complexes have low solubility, and hence if they are formed in the gel or boundary layer following contact of the ASD with buffer, a slow or non-existent dissolution rate will be observed. Furthermore, the pH in the boundary layer region is likely to be lower than the bulk solution pH, an important consideration when making predictions about drug ionization tendency based on the pK_a value. In contrast, most neutral or anionic drugs that we studied were found to have a lower impact on ASD release performance than cationic drugs, when compared at similar drug loadings. Future studies are needed to ascertain if these *in vitro* observations translate into poor *in vivo* performance.

7. Acknowledgements

We are grateful to Dmitry Zemlyanov for conducting XPS studies on tablets and help in interpretation of data. Boehringer Ingelheim Pharmaceuticals Inc. is thanked for providing

funding for this study. The National Science Foundation is acknowledged for funding (DMR-2204995).

ASSOCIATED CONTENT

Supporting Information

Composition of various buffer solutions, HPLC quantification methods for drugs, normalized released rates of drugs from select ASDs in 50 mM pH 6.8 phosphate buffer, HPMCAS complexation with LOR in buffers of various ionic strengths, PXRD and PLM images of ASDs confirming their amorphous nature.

.

8. References

(1) Beig, A.; Fine-Shamir, N.; Lindley, D.; Miller, J. M.; Dahan, A. Advantageous Solubility-Permeability Interplay When Using Amorphous Solid Dispersion (ASD) Formulation for the BCS Class IV P-Gp Substrate Rifaximin: Simultaneous Increase of Both the Solubility and the Permeability. *AAPS J* **2017**, *19* (3), 806–813. https://doi.org/10.1208/s12248-017-0052-1.

(2) Alonzo, D. E.; Zhang, G. G. Z.; Zhou, D.; Gao, Y.; Taylor, L. S. Understanding the Behavior of Amorphous Pharmaceutical Systems during Dissolution. *Pharm. Res.* **2010**, *27* (4), 608–618. https://doi.org/10.1007/s11095-009-0021-1.

(3) Chen, Y.; Wang, S.; Wang, S.; Liu, C.; Su, C.; Hageman, M.; Hussain, M.; Haskell, R.; Stefanski, K.; Qian, F. Initial Drug Dissolution from Amorphous Solid Dispersions Controlled by Polymer Dissolution and Drug-Polymer Interaction. *Pharm. Res.* **2016**, *33* (10), 2445–2458. https://doi.org/10.1007/s11095-016-1969-2.

(4) Huang, Y.; Dai, W.-G. Fundamental Aspects of Solid Dispersion Technology for Poorly Soluble Drugs. *Acta Pharm. Sin. B* **2014**, *4* (1), 18–25. https://doi.org/10.1016/j.apsb.2013.11.001.

(5) Harmon, P.; Li, L.; Marsac, P. J.; McKelvey, C.; Variankaval, N.; Xu, W. Amorphous Solid Dispersion: Analytical Chanllenges and Opportunities. *AAPS Newsmagazine* **2009**, *12*, 14–20.

(6) Curatolo, W. J.; Herbig, S. M.; Nightingale, J. A. S. Solid Pharmaceutical Dispersions with Enhanced Bioavailability. US8257741B2, September 4, 2012. https://patents.google.com/patent/US8257741B2/en (accessed 2022-03-06).

(7) Kennedy, M.; Hu, J.; Gao, P.; Li, L.; Ali-Reynolds, A.; Chal, B.; Gupta, V.; Ma, C.; Mahajan, N.; Akrami, A.; Surapaneni, S. Enhanced Bioavailability of a Poorly Soluble VR1 Antagonist Using an Amorphous Solid Dispersion Approach: A Case Study. *Mol. Pharmaceutics.* **2008**, *5* (6), 981–993. https://doi.org/10.1021/mp800061r.

(8) Brouwers, J.; Brewster, M. E.; Augustijns, P. Supersaturating Drug Delivery Systems: The Answer to Solubility-Limited Oral Bioavailability? *J. Pharm. Sci.* **2009**, *98* (8), 2549–2572. https://doi.org/10.1002/jps.21650.
(9) Raina, S. A.; Zhang, G. G. Z.; Alonzo, D. E.; Wu, J.; Zhu, D.; Catron, N. D.; Gao, Y.; Taylor, L. S. Enhancements and Limits in Drug Membrane Transport Using Supersaturated Solutions of Poorly Water Soluble Drugs. *J. Pharm. Sci.* **2014**, *103* (9), 2736–2748. https://doi.org/10.1002/jps.23826.
(10) Saboo, S.; Bapat, P.; Moseson, D. E.; Kestur, U. S.; Taylor, L. S. Exploring the Role of Surfactants in Enhancing Drug Release from Amorphous Solid Dispersions at Higher Drug Loadings. *Pharmaceutics.* **2021**, *13* (5), 735. https://doi.org/10.3390/pharmaceutics13050735.
(11) Chen, Y.; Liu, C.; Chen, Z.; Su, C.; Hageman, M.; Hussain, M.; Haskell, R.; Stefanski, K.; Qian, F. Drug–Polymer–Water Interaction and Its Implication for the Dissolution Performance of Amorphous Solid Dispersions. *Mol. Pharmaceutics.* **2015**, *12* (2), 576–589. https://doi.org/10.1021/mp500660m.
(12) Chavan, R. B.; Rathi, S.; Jyothi, V. G. S. S.; Shastri, N. R. Cellulose Based Polymers in Development of Amorphous Solid Dispersions. *Asian J. Pharm. Sci.* **2019**, *14* (3), 248–264. https://doi.org/10.1016/j.ajps.2018.09.003.
(13) Mosquera-Giraldo, L. I.; Borca, C. H.; Meng, X.; Edgar, K. J.; Slipchenko, L. V.; Taylor, L. S. Mechanistic Design of Chemically Diverse Polymers with Applications in Oral Drug Delivery. *Biomacromolecules* **2016**, *17* (11), 3659–3671. https://doi.org/10.1021/acs.biomac.6b01156.
(14) Hiew, T. N.; Zemlyanov, D. Y.; Taylor, L. S. Balancing Solid-State Stability and Dissolution Performance of Lumefantrine Amorphous Solid Dispersions: The Role of Polymer Choice and Drug–Polymer Interactions. *Mol. Pharmaceutics.* **2022**, *19* (2), 392–413. https://doi.org/10.1021/acs.molpharmaceut.1c00481.
(15) Indulkar, A. S.; Lou, X.; Zhang, G. G. Z.; Taylor, L. S. Insights into the Dissolution Mechanism of Ritonavir–Copovidone Amorphous Solid Dispersions: Importance of Congruent Release for Enhanced Performance. *Mol. Pharmaceutics.* **2019**, *16* (3), 1327–1339. https://doi.org/10.1021/acs.molpharmaceut.8b01261.
(16) Saboo, S.; Mugheirbi, N. A.; Zemlyanov, D. Y.; Kestur, U. S.; Taylor, L. S. Congruent Release of Drug and Polymer: A "Sweet Spot" in the Dissolution of Amorphous Solid Dispersions. *J. Controlled Release* **2019**, *298*, 68–82. https://doi.org/10.1016/j.jconrel.2019.01.039.
(17) Saboo, S.; Kestur, U. S.; Flaherty, D. P.; Taylor, L. S. Congruent Release of Drug and Polymer from Amorphous Solid Dispersions: Insights into the Role of Drug-Polymer Hydrogen Bonding, Surface Crystallization, and Glass Transition. *Mol. Pharmaceutics.* **2020**, *17* (4), 1261–1275. https://doi.org/10.1021/acs.molpharmaceut.9b01272.
(18) Deac, A.; Qi, Q.; Indulkar, A. S.; Purohit, H. S.; Gao, Y.; Zhang, G. G. Z.; Taylor, L. S. Dissolution Mechanisms of Amorphous Solid Dispersions: Role of Drug Load and Molecular Interactions. *Mol. Pharmaceutics.* **2023**, *20* (1), 722–737. https://doi.org/10.1021/acs.molpharmaceut.2c00892.
(19) Yang, R.; Mann, A. K. P.; Van Duong, T.; Ormes, J. D.; Okoh, G. A.; Hermans, A.; Taylor, L. S. Drug Release and Nanodroplet Formation from Amorphous Solid Dispersions: Insight into the Roles of Drug Physicochemical Properties and Polymer Selection. *Mol.*

Pharmaceutics. **2021**, *18* (5), 2066–2081. https://doi.org/10.1021/acs.molpharmaceut.1c00055.
(20) Yang, R.; Zhang, G. G. Z.; Zemlyanov, D. Y.; Purohit, H. S.; Taylor, L. S. Release Mechanisms of Amorphous Solid Dispersions: Role of Drug-Polymer Phase Separation and Morphology. *J. Pharm. Sci.* **2023**, *112* (1), 304–317. https://doi.org/10.1016/j.xphs.2022.10.021.
(21) Aakeröy, C. B.; Spartz, C. L.; Dembowski, S.; Dwyre, S.; Desper, J. A Systematic Structural Study of Halogen Bonding *versus* Hydrogen Bonding within Competitive Supramolecular Systems. *IUCrJ* **2015**, *2* (5), 498–510. https://doi.org/10.1107/S2052252515010854.
(22) Berger, G.; Soubhye, J.; Meyer, F. Halogen Bonding in Polymer Science: From Crystal Engineering to Functional Supramolecular Polymers and Materials. *Poly. Chem.* **2015**, *6* (19), 3559–3580. https://doi.org/10.1039/C5PY00354G.
(23) Chailu Que; Qi, Q.; Zemlyanov, D. Y.; Mo, H.; Deac, A.; Zeller, M.; Indulkar, A. S.; Gao, Y.; Zhang, G. G. Z.; Taylor, L. S. Evidence for Halogen Bonding in Amorphous Solid Dispersions. *Cryst. Growth Des.* **2020**, *20* (5), 3224–3235. https://doi.org/10.1021/acs.cgd.0c00073.
(24) Xu, Z.; Yang, Z.; Liu, Y.; Lu, Y.; Chen, K.; Zhu, W. Halogen Bond: Its Role beyond Drug–Target Binding Affinity for Drug Discovery and Development. *J. Chem. Inf. Model.* **2014**, *54* (1), 69–78. https://doi.org/10.1021/ci400539q.
(25) Robertson, C. C.; Wright, J. S.; Carrington, E. J.; Perutz, R. N.; Hunter, C. A.; Brammer, L. Hydrogen Bonding vs. Halogen Bonding: The Solvent Decides. *Chem. Sci.* **2017**, *8* (8), 5392–5398. https://doi.org/10.1039/C7SC01801K.
(26) Kothari, K.; Ragoonanan, V.; Suryanarayanan, R. The Role of Drug–Polymer Hydrogen Bonding Interactions on the Molecular Mobility and Physical Stability of Nifedipine Solid Dispersions. *Mol. Pharmaceutics.* **2015**, *12* (1), 162–170. https://doi.org/10.1021/mp5005146.
(27) Que, C.; Lou, X.; Zemlyanov, D. Y.; Mo, H.; Indulkar, A. S.; Gao, Y.; Zhang, G. G. Z.; Taylor, L. S. Insights into the Dissolution Behavior of Ledipasvir–Copovidone Amorphous Solid Dispersions: Role of Drug Loading and Intermolecular Interactions. *Mol. Pharmaceutics.* **2019**, *16* (12), 5054–5067. https://doi.org/10.1021/acs.molpharmaceut.9b01025.
(28) Saboo, S.; Moseson, D. E.; Kestur, U. S.; Taylor, L. S. Patterns of Drug Release as a Function of Drug Loading from Amorphous Solid Dispersions: A Comparison of Five Different Polymers. *Eur. J. Pharm. Sci.* **2020**, *155*, 105514. https://doi.org/10.1016/j.ejps.2020.105514.
(29) Qi, Q.; Taylor, L. S. Improved Dissolution of an Enteric Polymer and Its Amorphous Solid Dispersions by Polymer Salt Formation. *Int. J. Pharm.* **2022**, *622*, 121886. https://doi.org/10.1016/j.ijpharm.2022.121886.
(30) Delporte, J. P. [Enteric coating]. *Pharm. Acta. Helv.* **1970**, *45* (9), 525–552.
(31) Al-Gousous, J.; Ruan, H.; Blechar, J. A.; Sun, K. X.; Salehi, N.; Langguth, P.; Job, N. M.; Lipka, E.; Loebenberg, R.; Bermejo, M.; Amidon, G. E.; Amidon, G. L. Mechanistic Analysis and Experimental Verification of Bicarbonate-Controlled Enteric Coat Dissolution: Potential in Vivo Implications. *Eur. J. Pharm. Biopharm.* **2019**, *139*, 47–58. https://doi.org/10.1016/j.ejpb.2019.03.012.

(32) Al-Zoubi, N.; Al-Rusasi, A.; Sallam, A.-S. Ethanol Effect on Acid Resistance of Selected Enteric Polymers. *Pharm. Develop. Tech.* **2019**, *24* (1), 24–34. https://doi.org/10.1080/10837450.2017.1412461.
(33) Dangel C; Kolter K; Reich Hb; Schepky G. Aqueous Enteric Coatings with Methacryclic Acid Copolymer Type C. *Pharm. Technol. Eur.* 2000, 24 (4), 36−37.
(34) Davis, M.; Ichikawa, I.; Williams, E. J.; Banker, G. S. Comparison and Evaluation of Enteric Polymer Properties in Aqueous Solutions. *Int. J. Pharm.* **1986**, *28* (2), 157–166. https://doi.org/10.1016/0378-5173(86)90241-3.
(35) Harianawala, A. I. Investigation of Viscosity, pH and Dielectric Constant of the Microenvironment Surrounding a Dissolving Enteric Polymer Film. Ph.D. Thesis, University of Connecticut, United States, 2022.
(36) Ozturk, S. S.; Palsson, B. O.; Donohoe, B.; Dressman, J. B. Kinetics of Release from Enteric-Coated Tablets. *Pharm. Res.* **1988**, *5* (9), 550–565. https://doi.org/10.1023/A:1015937912504.
(37) J, S.; R, K. Factors Affecting the Dissolution Rate of Enteric Coatings. *Pharm. Ind.* **1977**, *39* (5), 502–505.
(38) Vodak, D. T.; Morgen, M. Design and Development of HPMCAS-Based Spray-Dried Dispersions. In *Amorphous Solid Dispersions: Theory and Practice*; Shah, N., Sandhu, H., Choi, D. S., Chokshi, H., Malick, A. W., Eds.; Advances in Delivery Science and Technology; Springer: New York, NY, 2014; pp 303–322. https://doi.org/10.1007/978-1-4939-1598-9_9.
(39) Curatolo, W.; Nightingale, J. A.; Herbig, S. M. Utility of Hydroxypropylmethylcellulose Acetate Succinate (HPMCAS) for Initiation and Maintenance of Drug Supersaturation in the GI Milieu. *Pharm. Res.* **2009**, *26* (6), 1419–1431. https://doi.org/10.1007/s11095-009-9852-z.
(40) Friesen, D. T.; Shanker, R.; Crew, M.; Smithey, D. T.; Curatolo, W. J.; Nightingale, J. A. S. Hydroxypropyl Methylcellulose Acetate Succinate-Based Spray-Dried Dispersions: An Overview. *Mol. Pharmaceutics.* **2008**, *5* (6), 1003–1019. https://doi.org/10.1021/mp8000793.
(41) Wan, L. S. C.; Heng, P. W. S.; Chia, C. G. H. Spray Drying as a Process for Microencapsulation and the Effect of Different Coating Polymers. *Drug Dev. Ind. Pharm.* **1992**, *18* (9), 997–1011. https://doi.org/10.3109/03639049209069311.
(42) Lu, X., Huang, C., Lowinger, M.B., Yang, F., Xu, W., Brown, C.D., Hesk, D., Koynov, A., Schenck, L., Su, Y. Molecular Interactions in Posaconazole Amorphous Solid Dispersions from Two-Dimensional Solid-State NMR Spectroscopy. *Mol. Pharmaceutics.* **2019**, 16, 6, 2579–2589 https://doi.org/10.1021/acs.molpharmaceut.9b00174.
(43) Song, Y.; Zemlyanov, D.; Chen, X.; Su, Z.; Nie, H.; Lubach, J. W.; Smith, D.; Byrn, S.; Pinal, R. Acid-Base Interactions in Amorphous Solid Dispersions of Lumefantrine Prepared by Spray-Drying and Hot-Melt Extrusion Using X-Ray Photoelectron Spectroscopy. *Int. J. Pharm.* **2016**, *514* (2), 456–464. https://doi.org/10.1016/j.ijpharm.2016.06.126.
(44) Harianawala, A. I.; Bogner, R. H.; Bradley, M. Measurement of pH near Dissolving Enteric Coatings. *Int. J. Pharm.* **2002**, *247* (1), 139–146. https://doi.org/10.1016/S0378-5173(02)00404-0.
(45) Karkossa, F.; Klein, S. Assessing the Influence of Media Composition and Ionic Strength on Drug Release from Commercial Immediate-Release and Enteric-Coated Aspirin Tablets. *J. Pharm. Pharmacol.* **2017**, *69* (10), 1327–1340. https://doi.org/10.1111/jphp.12777.

(46) Bapat, P.; Paul, S.; Thakral, N. K.; Tseng, Y.-C.; Taylor, L. S. Does Media Choice Matter When Evaluating the Performance of Hydroxypropyl Methylcellulose Acetate Succinate-Based Amorphous Solid Dispersions? *Mol. Pharmaceutics.* **2023**. https://doi.org/10.1021/acs.molpharmaceut.3c00586.
(47) Nguyen, H. T.; Van Duong, T.; Taylor, L. S. Impact of Gastric pH Variations on the Release of Amorphous Solid Dispersion Formulations Containing a Weakly Basic Drug and Enteric Polymers. *Mol. Pharmaceutics.* **2023**, *20* (3), 1681–1695. https://doi.org/10.1021/acs.molpharmaceut.2c00895.
(48) Ilevbare, G. A.; Taylor, L. S. Liquid–Liquid Phase Separation in Highly Supersaturated Aqueous Solutions of Poorly Water-Soluble Drugs: Implications for Solubility Enhancing Formulations. *Cryst. Growth Des.* **2013**, *13* (4), 1497–1509. https://doi.org/10.1021/cg301679h.
(49) Maghsoodi, M.; Astemal, S. M.; Nokhodchi, A.; Kiaie, H.; Khoshfetrat, A. B.; Talebi, F. An Insight into Eudragit S100 Preserving Mechanism of Cinnarizine Supersaturation. *AAPS PharmSciTech* **2022**, *23* (3), 80. https://doi.org/10.1208/s12249-022-02223-x.
(50) Morgan, E. M.; Lotfy, H. M.; Obaydo, R. H.; Fayez, Y. M.; Abdelkawy, M.; Boltia, S. A. Whiteness and Greenness Assessment with Efficacy Evaluation of Two UPLC Systems Applied for the Quantification of Cinnarizine and Dimenhydrinate along with Their Toxic Impurities. *Sustain. Chem. Pharm.* **2023**, *36*, 101225. https://doi.org/10.1016/j.scp.2023.101225.
(51) O'Brien, M.; McCauley, J.; Cohen, E. Indomethacin. In *Analytical Profiles of Drug Substances*; Florey, K., Ed.; Academic Press, 1984; Vol. 13, pp 211–238. https://doi.org/10.1016/S0099-5428(08)60192-6.
(52) Law, D.; Krill, S. L.; Schmitt, E. A.; Fort, J. J.; Qiu, Y.; Wang, W.; Porter, W. R. Physicochemical Considerations in the Preparation of Amorphous Ritonavir–Poly(Ethylene Glycol) 8000 Solid Dispersions. *J. Pharm. Sci.* **2001**, *90* (8), 1015–1025. https://doi.org/10.1002/jps.1054.
(53) Hsieh, Y.-L.; Ilevbare, G. A.; Van Eerdenbrugh, B.; Box, K. J.; Sanchez-Felix, M. V.; Taylor, L. S. pH-Induced Precipitation Behavior of Weakly Basic Compounds: Determination of Extent and Duration of Supersaturation Using Potentiometric Titration and Correlation to Solid State Properties. *Pharm. Res.* **2012**, *29* (10), 2738–2753. https://doi.org/10.1007/s11095-012-0759-8.
(54) Maghsoodi, M.; Nokhodchi, A.; Oskuei, M. A.; Heidari, S. Formulation of Cinnarizine for Stabilization of Its Physiologically Generated Supersaturation. *AAPS PharmSciTech* **2019**, *20* (3), 139. https://doi.org/10.1208/s12249-019-1338-7.
(55) Mehler, E. l.; Fuxreiter, M.; Simon, I.; Garcia-Moreno E, B. The Role of Hydrophobic Microenvironments in Modulating pKa Shifts in Proteins. *Proteins: Structure, Function, and Bioinformatics* **2002**, *48* (2), 283–292. https://doi.org/10.1002/prot.10153.
(56) Harris, T. K.; Turner, G. J. Structural Basis of Perturbed pKa Values of Catalytic Groups in Enzyme Active Sites. *IUBMB Life* **2002**, *53* (2), 85–98. https://doi.org/10.1080/15216540211468.
(57) D. Ristroph, K.; K. Prud'homme, R. Hydrophobic Ion Pairing: Encapsulating Small Molecules, Peptides, and Proteins into Nanocarriers. *Nanoscale Adv.* **2019**, *1* (11), 4207–4237. https://doi.org/10.1039/C9NA00308H.
(58) Song, Y. H.; Shin, E.; Wang, H.; Nolan, J.; Low, S.; Parsons, D.; Zale, S.; Ashton, S.; Ashford, M.; Ali, M.; Thrasher, D.; Boylan, N.; Troiano, G. A Novel in Situ Hydrophobic

Ion Pairing (HIP) Formulation Strategy for Clinical Product Selection of a Nanoparticle Drug Delivery System. *J. Controlled Release* **2016**, *229*, 106–119. https://doi.org/10.1016/j.jconrel.2016.03.026.
(59) Shahzadi, I.; Asim, M. H.; Dizdarević, A.; Wolf, J. D.; Kurpiers, M.; Matuszczak, B.; Bernkop-Schnürch, A. Arginine-Based Cationic Surfactants: Biodegradable Auxiliary Agents for the Formation of Hydrophobic Ion Pairs with Hydrophilic Macromolecular Drugs. *J. Colloid Interface Sci.* **2019**, *552*, 287–294. https://doi.org/10.1016/j.jcis.2019.05.057.
(60) Castro, G. A.; Coelho, A. L. L. R.; Oliveira, C. A.; Mahecha, G. A. B.; Oréfice, R. L.; Ferreira, L. A. M. Formation of Ion Pairing as an Alternative to Improve Encapsulation and Stability and to Reduce Skin Irritation of Retinoic Acid Loaded in Solid Lipid Nanoparticles. *Int. J. Pharm.* **2009**, *381* (1), 77–83. https://doi.org/10.1016/j.ijpharm.2009.07.025.
(61) Bussano, R.; Chirio, D.; Costa, L.; Turci, F.; Trotta, M. Preparation and Characterization of Insulin-Loaded Lipid-Based Microspheres Generated by Electrospray. *J Dispers. Sci. Technol*. **2011**, *32* (10), 1524–1530. https://doi.org/10.1080/01932691.2010.505876.
(62) Gaudana, R.; Gokulgandhi, M.; Khurana, V.; Kwatra, D.; Mitra, A. K. Design and Evaluation of a Novel Nanoparticulate-Based Formulation Encapsulating a HIP Complex of Lysozyme. *Pharm. Dev. Tech.* **2013**, *18* (3), 752–759. https://doi.org/10.3109/10837450.2012.737806.
(63) Cheow, W. S.; Hadinoto, K. Self-Assembled Amorphous Drug–Polyelectrolyte Nanoparticle Complex with Enhanced Dissolution Rate and Saturation Solubility. *J. Col. Int. Sci.* **2012**, *367* (1), 518–526. https://doi.org/10.1016/j.jcis.2011.10.011.
(64) Dong, B.; Hadinoto, K. Amorphous Nanoparticle Complex of Perphenazine and Dextran Sulfate as a New Solubility Enhancement Strategy of Antipsychotic Perphenazine. *Drug Dev. Ind. Pharm.* **2017**, *43* (6), 996–1002. https://doi.org/10.1080/03639045.2017.1287721.
(65) Gaudana, R.; Parenky, A.; Vaishya, R.; Samanta, S. K.; Mitra, A. K. Development and Characterization of Nanoparticulate Formulation of a Water Soluble Prodrug of Dexamethasone by HIP Complexation. *J. Microencapsul.* **2011**, *28* (1), 10–20. https://doi.org/10.3109/02652048.2010.520093.
(66) Goddard, E. D.; Hannan, R. B. Cationic Polymer/Anionic Surfactant Interactions. *J. Col. Int. Sci.* **1976**, *55* (1), 73–79. https://doi.org/10.1016/0021-9797(76)90010-2.
(67) Caram-Lelham, N.; Hed, F.; Sundelöf, L.-O. Adsorption of Charged Amphiphiles to Oppositely Charged Polysaccharides—A Study of the Influence of Polysaccharide Structure and Hydrophobicity of the Amphiphile Molecule. *Biopolymers.* **1997**, *41* (7), 765–772. https://doi.org/10.1002/(SICI)1097-0282(199706)41:7<765::AID-BIP5>3.0.CO;2-N.
(68) Johnson, N. R.; Wang, Y. Coacervate Delivery Systems for Proteins and Small Molecule Drugs. *Expert Opin. Drug Deliv.* **2014**, *11* (12), 1829–1832. https://doi.org/10.1517/17425247.2014.941355.
(69) Overbeek, J. T. G.; Voorn, M. J. Phase Separation in Polyelectrolyte Solutions. Theory of Complex Coacervation. *J. Cell. Comp. Physiol.* **1957**, *49* (S1), 7–26. https://doi.org/10.1002/jcp.1030490404.
(70) Gucht, J. van der; Spruijt, E.; Lemmers, M.; Cohen Stuart, M. A. Polyelectrolyte Complexes: Bulk Phases and Colloidal Systems. *J. Col. Int. Sci.* **2011**, *361* (2), 407–422. https://doi.org/10.1016/j.jcis.2011.05.080.

(71) Goddard, E. D.; Leung, P. S. Interaction of Cationic Surfactants with a Hydrophobically Modified Cationic Cellulose Polymer. *Langmuir* **1992**, *8* (5), 1499–1500. https://doi.org/10.1021/la00041a042.
(72) García-Soto, J.; Fernández, M. S. The Effect of Neutral and Charged Micelles on the Acid-Base Dissociation of the Local Anesthetic Tetracaine. *Biochim. Biophys. Acta (BBA) - Biomembr.* **1983**, *731* (2), 275–281. https://doi.org/10.1016/0005-2736(83)90019-6.
(73) Hayakawa, K.; Santerre, J. P.; Kwak, J. C. T. Study of Surfactant-Polyelectrolyte Interactions. Binding of Dodecyl- and Tetradecyltrimethylammonium Bromide by Some Carboxylic Polyelectrolytes. *Macromolecules* **1983**, *16* (10), 1642–1645. https://doi.org/10.1021/ma00244a017.
(74) Nazir, I.; Shahzadi, I.; Jalil, A.; Bernkop-Schnürch, A. Hydrophobic H-Bond Pairing: A Novel Approach to Improve Membrane Permeability. *Int. J. Pharm.* **2020**, *573*, 118863. https://doi.org/10.1016/j.ijpharm.2019.118863.
(75) Kunimitsu, D. K.; Woody, A. Y.; Stimson, E. R.; Scheraga, H. A. Thermodynamic Data from Fluorescence Spectra. II. Hydrophobic Bond Formation in Binary Complexes. *J. Phys. Chem.* **1968**, *72* (3), 856–866. https://doi.org/10.1021/j100849a014.